Caving 2010 — Y. Potvin (ed)

https://papers.acg.uwa.edu.au/p/1002_33_Potvin/

Interpretation of seismic data and numerical modelling of fault reactivation at El Teniente, Reservas Norte sector

Y. Potvin *Australian Centre for Geomechanics, The University of Western Australia, Australia*

J. Jarufe *Codelco Chile, Chile*

J. Wesseloo *Australian Centre for Geomechanics, The University of Western Australia, Australia*

Abstract

Reservas Norte (RENO) is one of the panel caving sectors of El Teniente mines, owned by Codelco Chile. The sector has experienced mine-induced seismicity for many years. The work presented in this paper focusses on seismic activity recorded between the period from January 2004 to July 2008. The interpretation of the seismic data revealed that the sources of elevated seismic hazard (large events) at RENO during this period could be attributed to four major geological structures: Falla G, Falla F, Falla C, Falla N1. In particular, the seismic response of the four structures to undercut blasting activities is examined in detail.

The use of numerical modelling has shown that it is possible to simulate this response after calibrating the model against the cumulative seismic moment released by the faults, as mining advances towards them. This calibrated numerical model can then be used to forecast future seismic responses. The main product of this work is a tool that can be used to rank different undercutting rates and geometries in terms of seismic hazard.

1 Introduction

El Teniente, owned by Codelco Chile, is the largest underground mine in the world producing 140,000 tpd. The main mining method used at El Teniente is panel caving. Current production comes from a number of sectors including Esmeralda, Diablo Regimiento and RENO. Each of these sectors can be considered a very large mine in its own right, producing between 30,000–45,000 tpd. The RENO sector was particularly affected by mine-induced seismicity since early 2000. The serious impact of seismicity at the RENO sector is worded by Oraneda and Sougarret (2007) as follows:

> *"A series of rockburst since 2001 slowed the pace of the advance of the cave, and a big rockburst in August 2005, forced us to review the way the sector was planned to be mined."*

Seismicity at the RENO sector is the subject of this paper. More specifically, the paper presents an interpretation of the seismic data recorded between January 2004 and July 2008, relating most of the large seismic events to four major geological structures (faults). This interpretation serves as the basis for numerical modelling, which after establishing correlations between the numerical and monitored seismic parameters, is to be used in the future as a planning tool to study undercut advance options that will minimise seismic hazard from fault slip mechanism.

2 Identification of the main seismic sources at RENO

Seismicity is not a random phenomenon. It is the result of a localised failure mechanism and therefore, seismic events can be related to a specific seismic source. The authors define a seismic source as a location where a mine-induced change in the stress field combines with a geological feature(s), (it could be discontinuities or lithologies) to produce a violent failure process. Such a failure process associated with a seismic source can take place over long periods of time, at least as long as mining changes the stress conditions.

Some seismic sources have the capacity to store and release large quantities of seismic energy (large magnitude events), producing from time to time periods of elevated seismic hazard and potentially high seismic risks.

In a preliminary analysis of the RENO seismic data (2004–2008), Heal (2008) associated some of the recorded seismicity to major faults systems (Figure 1).

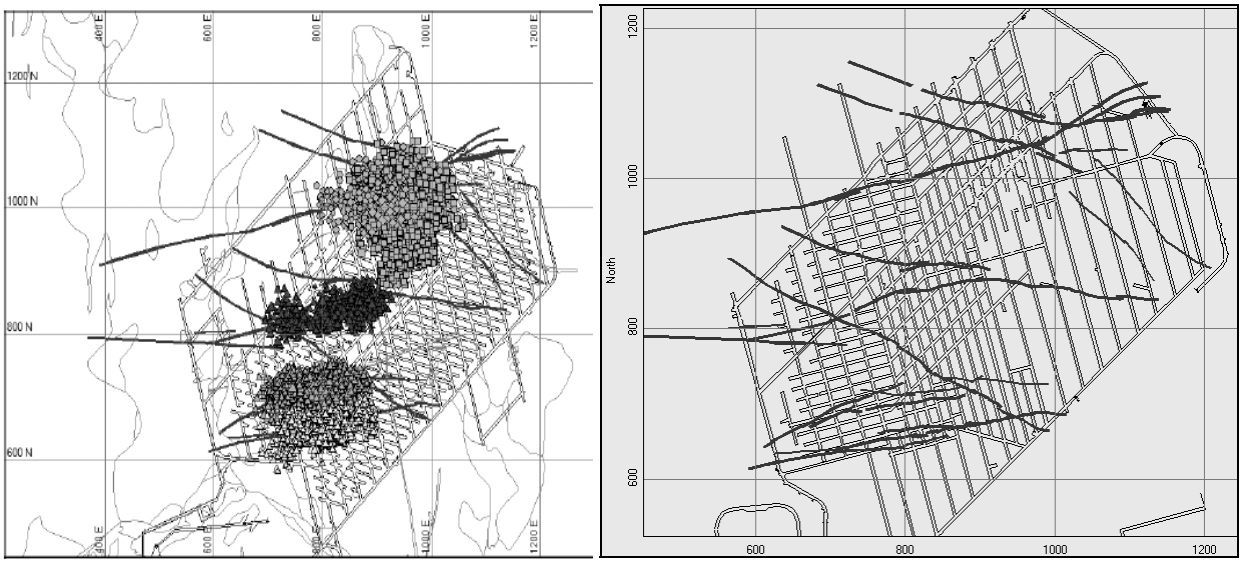

Figure 1 Plot of 33 cluster groups (left) at RENO compared to the location of faults (right)

Figure 2 shows the location of the significant events (events of local magnitude ≥ 0) that occurred between 2004 and 2008. The seven events shown on the east abutment are associated with the general increasing abutment stress rather than a response to the mining advance which progresses towards the west. As such, they are ignored from the analysis. Of the remaining significant events, 90% occurred within the encircled areas in Figure 2 located in the vicinity of Faults G, F, C and N1. These four faults are therefore interpreted as being the seismic sources responsible for the majority of high seismic risk at RENO.

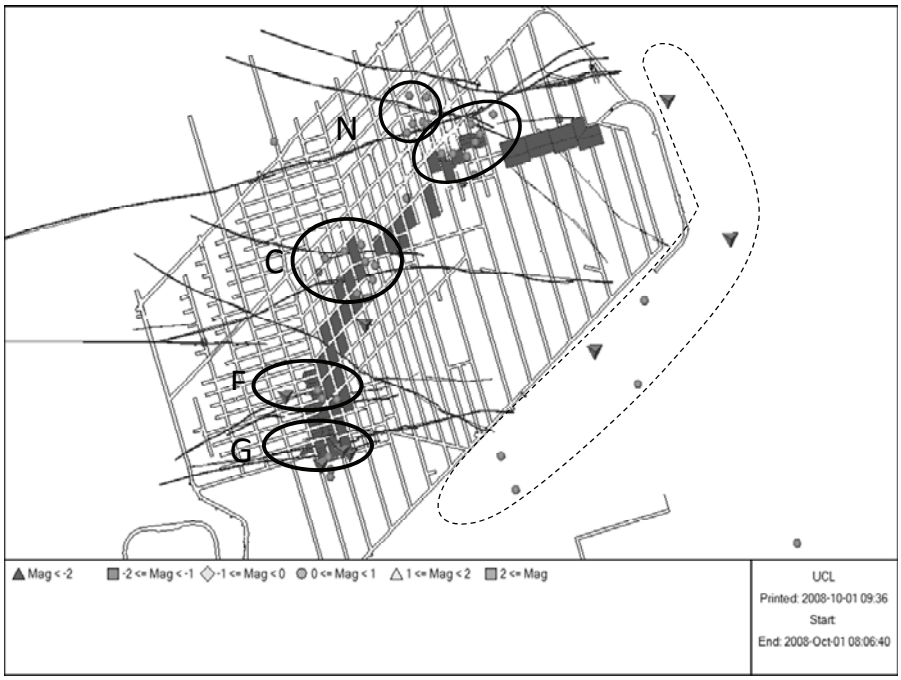

Figure 2 90% of all large events (ignoring the eastern abutment (dashed line)) occur within the circles and are coincident with Faults G, F, C and N1

The analysis of the S- to P-wave energy ratio of the seismic events belonging to the four faults is also supporting the above fault slip interpretation. Boatwright and Fletcher (1984) found that fault slip events in

general have significantly more energy in the (shear) S-wave when compare to the (compression) P-wave and (Cichowicz et al., 1990) suggest that an S- to P-energy ratio of 10 and more is indicative of a fault slip mechanism. On average, the S- to P-ratio of all events associated with the four faults of interest at RENO is approximately 23. Furthermore, over 70% of these events have a ratio above 10. This strongly supports the interpretation that these seismic sources have a fault slip shearing mechanism.

3 Seismic response of the major faults

It is informative to look at a cross-section along any of the faults (which are subvertical) to observe the vertical distribution of the seismicity (Figure 3). Clearly, the seismicity lines up on the west side of the cave, which is the direction of advance. Three seismic zones are delineated, and each of them is interpreted as a failure process specific to cave mining.

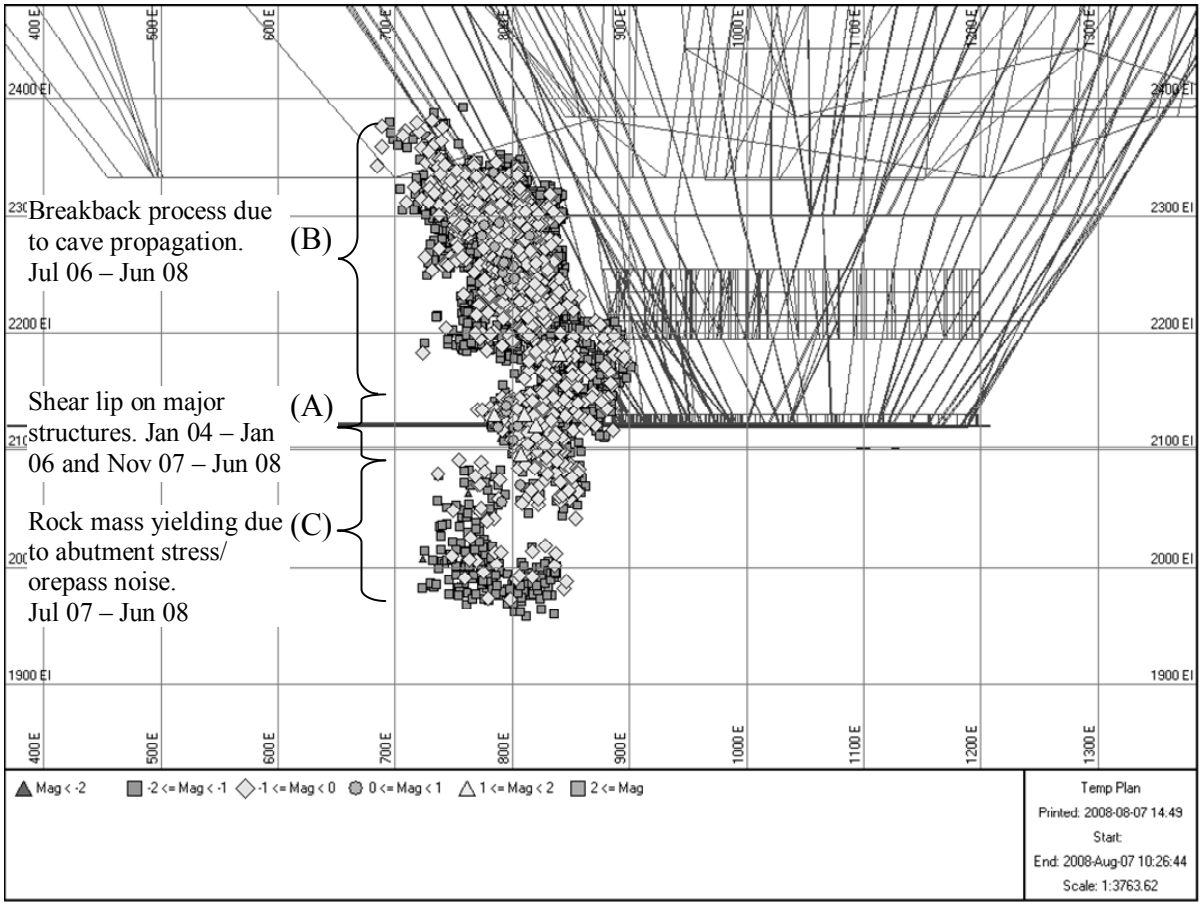

Figure 3 Cross-section looking north showing the three zones of seismicity associated with Fault G

Area A is approximately a 50 m thick slice extending 20 m above and 30 m below the undercut. Many of the significant events (magnitude ≥ 0) occur within this area. This is shown in Figure 4 where the number of significant events is plotted according to the elevation. The undercut level is indicated by the middle dashed line and is approximately at elevation 2,120 m. Keeping in mind that the precision of event location from historical data at RENO can be variable, the graph still indicates that many of the large events are somewhat close in elevation to the undercut and production levels. In reality they could well be a bit below the production level as large events in the past have caused damage to the floor of the production level.

Seismicity at RENO has a strong spatial and temporal relationship with undercut blasting activity nearby. This is shown in Figure 5, which provides an example of the seismic response to undercut advance. The dominant failure mechanism in this area is interpreted as being the fault slipping ahead of the advancing undercut.

The strong correlation between the significant seismic events and the undercut advances is further demonstrated in Figure 6, where the cumulative undercut blasted area are read on the left Y-axis and the cumulative number of significant seismic events are read on the right side Y-axis, both plotted against time.

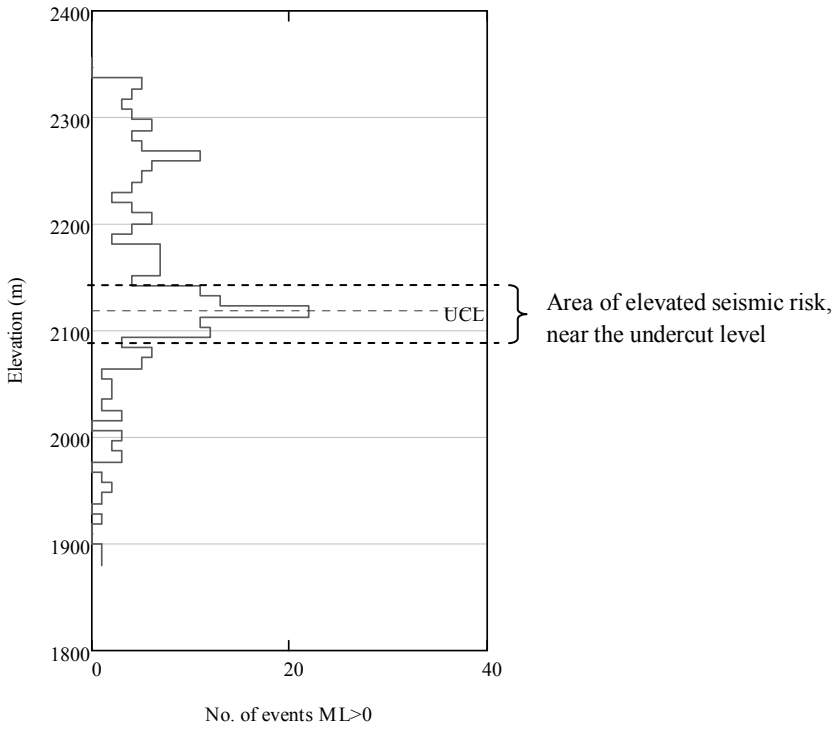

Figure 4 Distribution of events with local magnitude (M_L) larger than 0 shown as a function of their elevation

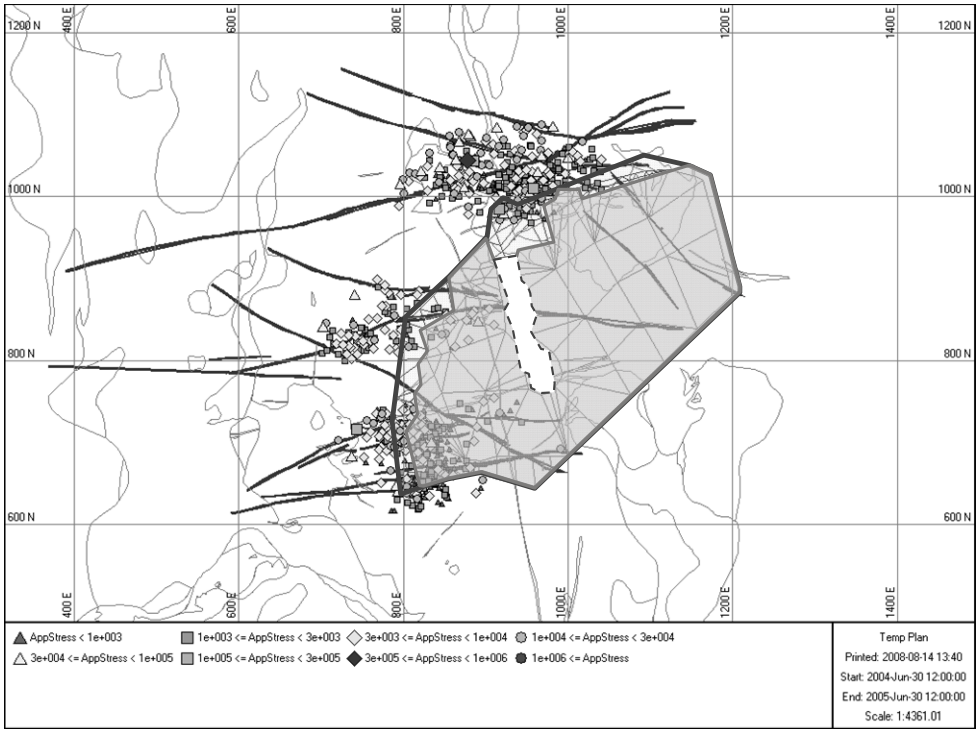

Figure 5 Seismic activity in Area A (near the undercut) associated with the undercut advance shown in dark, between June 2004 and June 2005

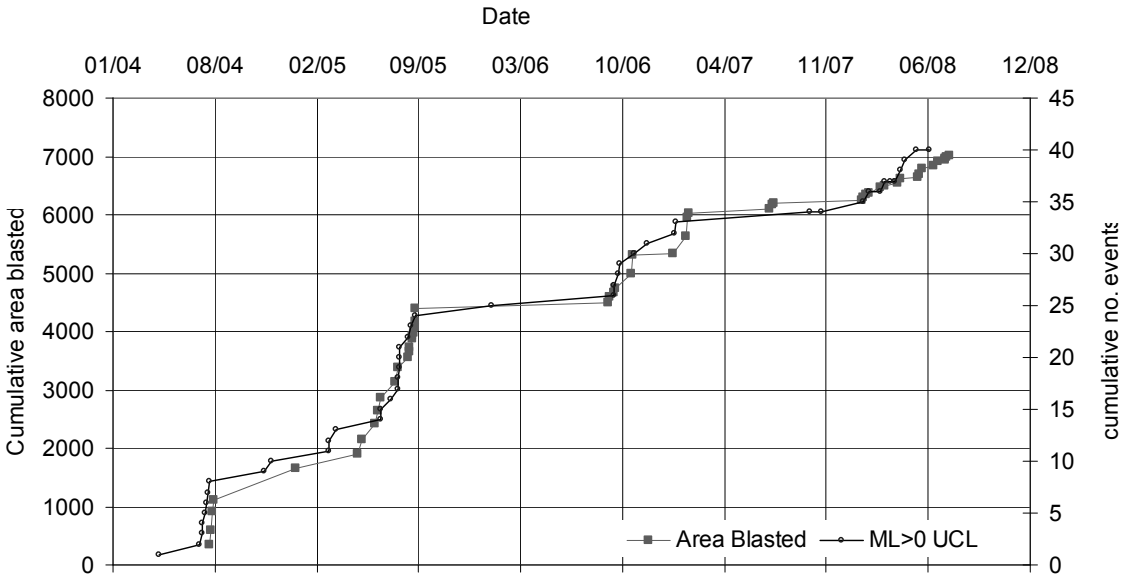

Figure 6 Cumulative undercut area blasted (large squares) compared to the cumulative number of significant events (dark line with small circles) showing a very strong correlation (drawbell blasts and event directly following those blasts were excluded from this analysis)

Area B is overlying area A and is believed to be associated with the cave expanding laterally and upwards, also labelled is the break-back process. Presumably, the break-back progresses as a response to both the undercut advances and the production (pulling ore from the drawpoints). Some large events are associated with the break-back process, but the risk associated with these events is lessened due to the long distance between the events and the location where mine workers' activities occur.

The seismic activity in Area C is located under the production area and could be caused by the abutment stress under the cave. Like the seismicity in Area B, the distance from workers' activity reduces the consequence of any significant events which occur in Area C.

These three distinct zones have been observed in all four seismic groups associated with Faults G, F, C and N1, and the highest risk comes from significant events located near the undercut and production levels, in Area A.

4 Numerical modelling approach of the fault slip mechanism

The major sources of high seismic hazard appear to be shear-slip on faults ahead of the undercut caused by stress changes due to the undercutting and caving processes. The seismic moment occurring on these faults is related to the displacement on the fault as:

$$M_o = G \cdot A \cdot D \quad (1)$$

Where G is the shear modulus; A is the area of slip; and D is the mean shear displacement. The slip on the structure can explicitly be modelled and the total cumulative moment calculated from this. This can be done in MAP3D by modelling the faults with displacement discontinuity (DD) elements and allowing plastic deformation on these elements. The modelled seismic moment associated with the slip occurring on the structure in a particular area is calculated as:

$$M_{o\ model} = G \cdot A \cdot D = G \cdot \sum_i a_i \cdot d_i \quad (2)$$

Where G, A, D are the modelled values of the shear modulus, the modelled area of slip and mean modelled slip. For a discretised plane the total moment can be obtained by summing the moment for each element, i, in the area of interest.

Low seismic efficiency, limited system sensitivity, model inaccuracy as well as the assumed shear strength of the structure will result in differences in the recorded and modelled moment.

5 Methodology employed to calibrate the fault slip model at RENO

The methodology adopted to calibrate the fault slip model against seismic data at RENO is based on the seismic moment, as described previously, and employs the following six steps.

5.1 Model selection and problem definition

As the main source of seismic hazard was identified as being a fault slip mechanism, the modelling tool to be used must allow for plastic deformation along a discontinuity. Because MAP3D is already extensively used at El Teniente Division, this program was selected as the preferred tool for this exercise, with its non-linear DD option to model the slipping mechanism along the predefined faults.

It was decided to calibrate the model based on three of the major faults at RENO. Faults G and N1 were selected because they are perhaps the most relevant faults in terms of their high seismic activity. Fault C was also modelled to obtain a comparison with a fault experiencing a lower level of seismicity.

As described in Section 4, the seismic parameter better suited to calibrate fault slip mechanism is the seismic moment, as it is directly dependent on the fault displacement, which can be calculated from MAP3D modelling. Based on the seismic monitoring data, the cumulative seismic moment was calculated for the three selected faults and graphically presented in Figure 7.

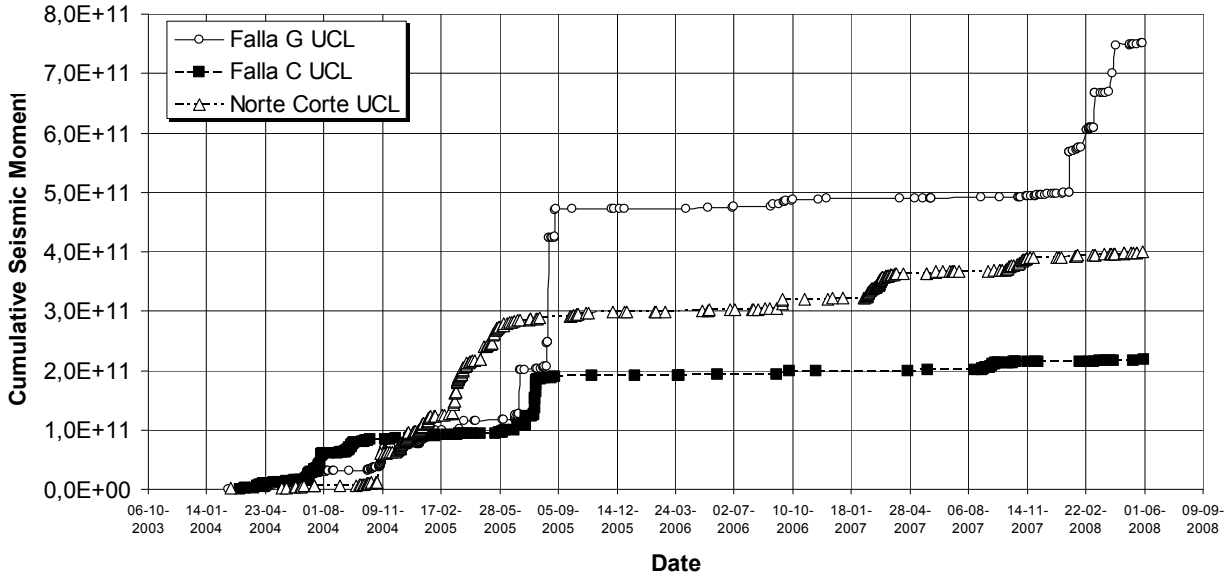

Figure 7 Cumulative seismic moment in selected faults at RENO Sector

5.2 Simplification of the model geometry

The mining method at El Teniente's RENO Sector is known as panel caving with advanced and conventional undercut. In this method, a low draw rate zone is implemented immediately behind the undercut. The drawbell extraction rate is reduced in this zone to control seismicity generated by stress readjustment, rock breakage and loosening. Behind this zone and further under the caved area, a free draw rate zone is allowed because it is believed that this has a minimum impact of local stress change and seismicity. The free draw under the cave will, however, move the broken material and generate a subsidence cone propagating to higher elevations (Figure 8).

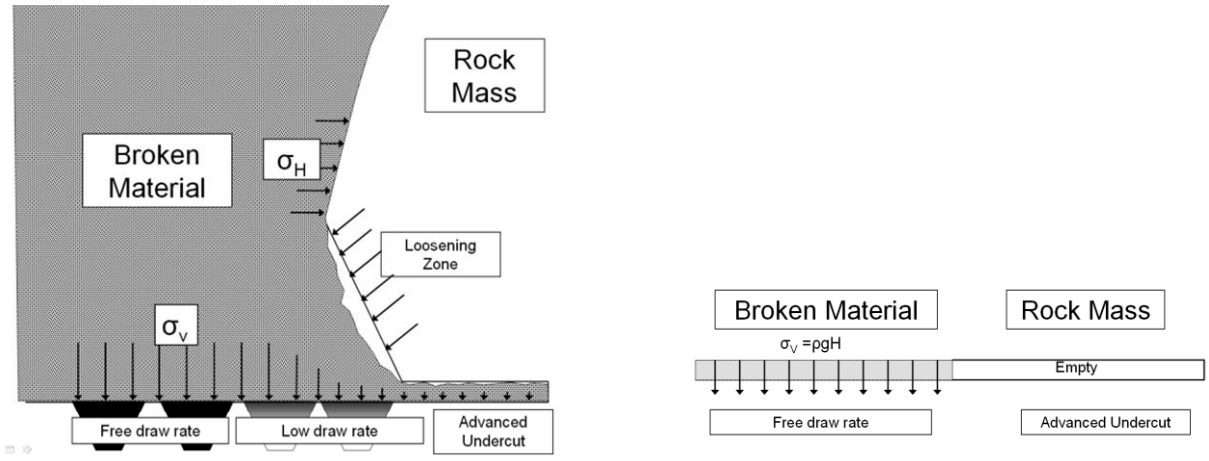

(a) (b)

Figure 8 (a) conceptual picture of the advanced undercut mining method (Jarufe, 2008); (b) simulation of the mining geometry considered for numerical modelling

Block caving methods are geomechanically complex and difficult to model. Ideally, one would like to simulate the various states of the rock mass existing at different locations (Figure 8), including the unaffected rock mass, the broken material and the loosening zone. To develop such a model would however, be beyond the capability of the hardware, the software and time frame available to this project. Furthermore, the real geometry above the undercut level is an inferred geometry which cannot be physically verified. The only parameter that is really well defined and controlled by the mine operation is the undercut geometry and the sequence of extraction. Therefore, some simplification and assumptions were necessary to construct a model that could be run easily using commonly available hardware in a practical timeframe.

Based on the previous discussion in Section 3, it was found that the high hazard seismicity is responding principally to undercut blasting. As such, the models constructed consider only the undercut geometry, using numerical approximation to simulate the effect of the broken material load at the point of extraction. A vertical load below the undercut level was assigned. This load effectively increases confinement at certain points behind the undercutting front and is taken as the boundary of the area of fault slip. This simplified way to model the broken rock allows for many test runs to be performed in a matter of hours compared to detailed modelling, which would take days to construct and weeks to run.

5.3 Regional model reliability assessment

A regional scale MAP3D model encompassing an area of 2 × 2 km was built. The reliability of this model was tested against three datasets. The model results were first compared with pre-mining stress measurements (20 measurements) performed away from mining influences. The model error against this dataset was approximately 27%.

The mine scale model was also compared with 133 historical stress measurements performed in all mine sectors, where the stress field was influenced by mining. Against this dataset, the model error was estimated to be within 37% of the measurements. In all stress measurements, the whole stress tensor was considered.

Finally, observational data on drifts overbreak at different levels of the RENO sector was also used for calibrating the regional model. When comparing with drift overbreak, the error between modelled and real data was estimated to be within 18%.

5.4 Defining faults and rock mass properties

For this study, only one lithology was considered and it is locally known as CMET, which corresponds to an andesite with strength and elastic properties as shown in Table 1 (after Celhay et al., 2005). As the rock mass is considered elastic in this analysis, only elastic parameters E and μ were utilised as rock mass properties in this study. The strength parameters are provided for reference purposes.

Table 1 Strength properties for RENO sector (Celhay et al., 2005)

Strength Properties	
Uniaxial compression (MPa)	65
Tensile strength (MPa)	5
Cohesion (MPa)	15
Friction angle (°)	35
Elastic Properties	
(μ) Poisson's ratio	0.2
(E) Young's modulus (GPa)	45

There were no strength tests available to define the properties of the three faults considered in this study. Trial runs involving generic values of strength parameters obtained from benchmarking studies (Karzulovick, 2001) were performed, but the results were not satisfactory when compared to the expected displacements along the faults experiencing high seismicity. Since the stress values given by the regional model were considered realistic based on the calibration work described in Section 5.3, the logical way to proceed was to modify fault properties based on parametric studies, until realistic answers were obtained.

The initial faults strength and elastic parameters selected for the model were defined as those that give a stable state to the fault in a pre-mining stress condition (Figure 9). The properties defined for this condition are admittedly low compared to benchmarked values. This was a conscious decision with the purpose of making potential fault slip calculations in the model more sensitive to small mining geometry changes. This is desirable since relatively small changes in the undercut geometry have produced significant release in terms of seismic moments. The residual properties of the fault were defined as equal to the peak properties, which produces elastic perfectly plastic behaviour.

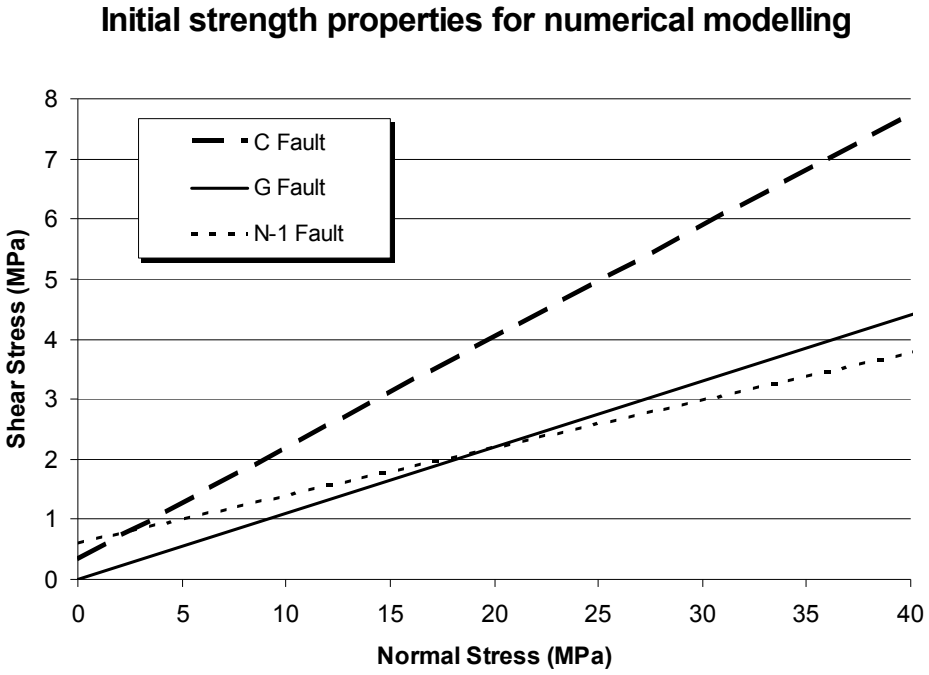

Figure 9 Initial strength properties defined for faults

5.5 Modelling mining stages

The main objective of the modelling work is to simulate the seismic response of faults caused by the mining activity, more specifically in this case, the undercutting geometry and rate. To select appropriate mining

steps and undercut geometries it is important that the model shows steps that produced high seismicity, but also, it is equally important that the model shows steps when the seismicity was low. Therefore, the stages of mining were selected based on the cumulative seismic moment graph (Figure 7) to represent periods of high and low seismic activity. The key mining steps (stages) selected for modelling are shown in Figure 10.

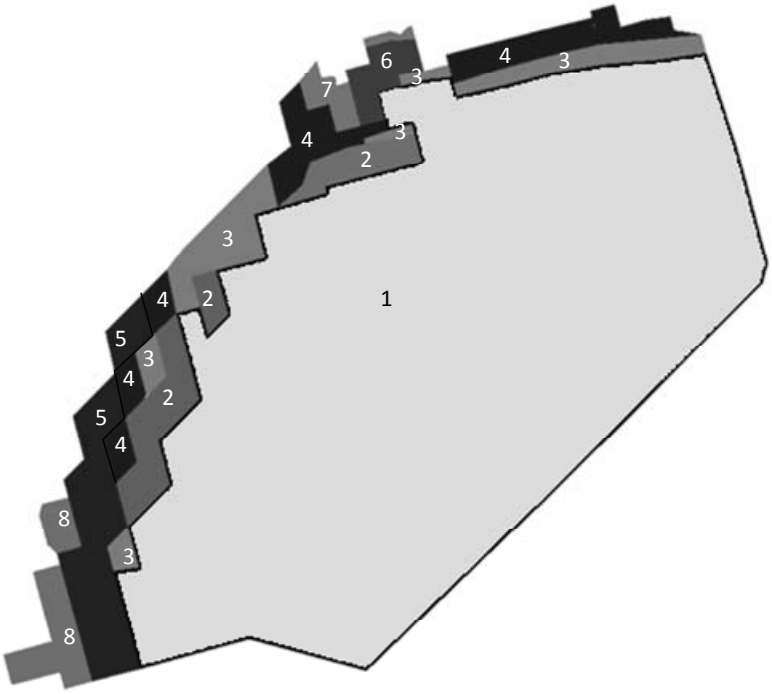

Figure 10 Mining stages for the modelling of the faults in the RENO sector

5.6 Analysis of the results

The model is essentially an undercut slot in a continuous rock mass, with a simulated zone of overlying broken rock and intersected by different planar discontinuities that represent the faults. The mining sequence considers the undercut advance from years 2002–2008, using the steps defined in the previous section. The main output from the modelled faults is the plastic displacement on the modelled faults. Considering the plastic displacement and the area of the fault being displaced, one can calculate a modelled seismic moment with Equation (2).

However, when calculated directly using Equation (2), the modelled seismic moment values were found to be very high. This is due to the low strength properties originally defined to produce stable faults in pre-mining stress state. To compensate this initial properties assumption, a scaling factor of 0.15 was applied to all the results (all faults were scaled by the same factor of 0.15). The results after scaling are shown in Figure 11, which compares well to the values from seismic monitoring shown in Figure 7.

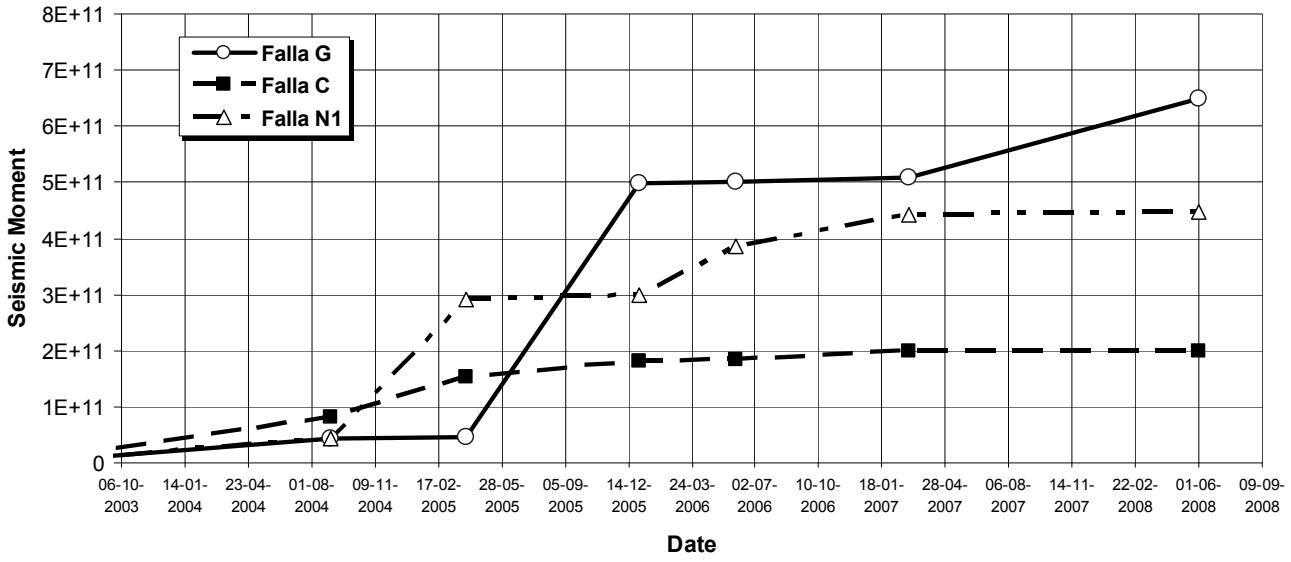

Figure 11 Cumulative scaled modelled seismic moment

At first glance, a good correlation is found between modelled seismic moment and seismic moment calculated from seismic data. To evaluate the reliability of the model, the cumulative seismic moments from individual faults were compared to the modelled values. The standard deviations and coefficient of variations are given in Table 2. These results are deemed acceptable considering the simplification and assumptions used in the model, and the usual deviation expected from modelling such a complicated problem.

Table 2 Correlation statics of the measured and modelled cumulative moment after applying a scaling factor of 0.15

Fault	Standard Deviation	Coefficient of Variation
C	2.72E+10	17%
G	5.32E+10	14%
N1	6.81E+10	26%

6 Summary and conclusion

The RENO sector of the El Teniente Mine has historically experienced seismicity problems. An analysis of the seismic data recorded between 2004 and 2008 showed that most of the seismic hazard and seismic risk in this sector can be attributed to four faults. More specifically, most of the hazardous significant events occur within a 50 m slice encompassing the undercut and the production level. These events are generally triggered by advancing (blasting) the undercut in the vicinity of the four faults.

A simplified numerical model was developed to calculate the potential seismic response of the faults to the undercut advance. After the encouraging results obtained through this study, the model will be further developed and the calibration refined. The calibrated numerical model is to be used in the future as a planning tool to study undercut advance options that will minimise seismic hazard from fault slip mechanisms.

The MAP3D program using the non-linear displacement discontinuity option was selected to comply with the hardware limitation and time constraint. The cave mining problem to be modelled was geomechanically complicated and required simplification. Despite the relatively simple model used, which contained assumptions regarding fault properties and mining geometry, the level of correlation between the modelled seismic moment and the values calculated from seismic monitoring data were within the expected accuracy, which allows for practical decisions to be made. Importantly, the model can be run rapidly on a PC at a very low cost.

This methodology has a very valuable application in the evaluation of undercutting geometries for future projects, as it would be possible to anticipate high seismicity periods and the zones potentially affected.

Acknowledgements

The authors wish to thank Codelco El Teniente Division for granting permission to publish this paper and the New Mine Level Project for funding this study.

References

Boatwright, J. and Fletcher, J.B. (1984) The partition of radiated energy between P and S waves, Bulletin of the Seismological Society of America, Vol. 74, pp. 361–376.

Celhay, F., Pereira, J. and Burgos, L. (2005) Geology and Resources for the New Mine Level, Pre-feasibility Engineering stage, SGL-I-030/05, Internal report Codelco-Chile.

Cichowicz, A., Green, R.W.E., Brink, A.v.Z., Grobler, P. and Mountfort, P.I. (1990) The space and time variation of micro-event parameters occurring in front of an active stope, in Proceedings Rockbursts and Seismicity in Mines, C. Fairhurst (ed), Minneapolis, Rotterdam, A.A. Balkema, pp. 171–175.

Heal, D. (2008) El Teniente Site Visit Summary, Mine Seismicity and Rockburst Risk management Project Phase 3, Internal report, Australian Centre for Geomechanics, Perth, Australia.

Jarufe, J. (2008) Methodology for the development of a mine scale 3D stress model for the New Mine Level Project, University of Santiago, Chile, Thesis Work (in Spanish).

Karzulovik, A. (2001) Geomechanics properties for primary rock discontinuities, AKL & Assoc. Ltda.

Oraneda, O. and Sougarret, A. (2007) Lessons learned in caving mining in hot rock, in Proceedings First International Seminar on Block and Sub-level Caving, The Southern Institute of Mining and Metallurgy, Johannesburg, South Africa, pp. 59–71.